
Deltahedral Views of Fullerene Polymorphism

Donald L. D. Caspar

Phil. Trans. R. Soc. Lond. A 1993 **343**, 133-144

doi: 10.1098/rsta.1993.0047

Email alerting service

Receive free email alerts when new articles cite this article - sign up in the box at the top right-hand corner of the article or click [here](#)

To subscribe to *Phil. Trans. R. Soc. Lond. A* go to:
<http://rsta.royalsocietypublishing.org/subscriptions>

Deltahedral views of fullerene polymorphism

BY DONALD L. D. CASPAR

*Rosenstiel Basic Medical Sciences Research Center and Department of Physics,
Braideis University, Waltham, Massachusetts 02254-9110, U.S.A.*

Fullerenes and icosahedral virus particles share the underlying geometry applied by Buckminster Fuller in his geodesic dome designs. The basic plan involves the construction of polyhedra from 12 pentagons together with some number of hexagons, or the symmetrically equivalent construction of triangular faceted surface lattices (deltahedra) with 12 five-fold vertices and some number of six-fold vertices. All the possible designs for icosahedral viruses built according to this plan were enumerated according to the triangulation number $T = (h^2 + hk + k^2)$ of icosadeltahedra formed by folding equilateral triangular nets with lattice vectors of indices h, k connecting neighbouring five-fold vertices. Lower symmetry deltahedra can be constructed in which the vectors connecting five-fold vertices are not all identical. Applying the pentagon isolation rule, the possible designs for fullerenes with more than 20 hexagonal facets can be defined by the set of vectors in the surface lattice net of the corresponding deltahedra. Surface lattice symmetry and geometrical relations among fullerene isomers can be displayed more directly in unfolded deltahedral nets than in projected views of the deltahedra or their hexagonally and pentagonally facted dual polyhedra.

1. Introduction

Buckminster Fuller (1963) called his discipline ‘comprehensive anticipatory design science’. Anticipatory science involves recognizing evident answers to questions that have not yet been asked. Fuller’s dymaxion geometry (cf. Marks 1960) started with his rediscovery of the cuboctahedron as the coordination polyhedron in cubic close packing, which he renamed the ‘vector equilibrium’. Visualizing this figure not as a solid but as a framework of edges connected at the vertices, he transformed the square faces into pairs of triangles to form an icosahedron; and subtriangulation of the spherical icosahedron led to his frequency modulated geodesic domes. Some of Fuller’s icosageodesic designs have been used for centuries in the Far East for weaving coolie hats (cf. Pawley 1962). Also anticipating geodesic dome designs, a complete enumeration of all possible subtriangulated icosahedral surface lattices (including chiral plans not used by Fuller) had been described by Goldberg (1937) as a mathematical curiosity. Inspired by Fuller’s dome designs, this enumeration was discovered again to explain why isometric virus particles have icosahedral symmetry (Caspar & Klug 1962). Following Fuller’s packing notions, Mackay (1962) arranged spherical particles on nested icosahedral surface lattice nets in a non-crystallographic packing which anticipated quasi-crystals. When Kroto *et al.* (1985) discovered C_{60} , which they modelled as the archimedean truncated icosahedron – the familiar football shape and Fuller’s lowest frequency modulated icosageodesic sphere – they appropriately named this anticipated structure ‘buckminsterfullerene’.

Phil. Trans. R. Soc. Lond. A (1993) **343**, 133–144

Printed in Great Britain

© 1993 The Royal Society

133

The essential characteristic of fullerenes is that each carbon atom is bonded to three neighbours forming a polyhedral shell with 12 pentagonal and some number of hexagonal facets; for C_{60} , there are 20 hexagonal facets. Possible isomers for higher fullerenes have been enumerated by Fowler, Manolopoulos and colleagues (Fowler, this volume; Fowler *et al.* 1991; Manolopoulos 1991; Manolopoulos & Fowler 1992); and some of the higher fullerenes have been isolated and spectroscopically characterized (Diederich *et al.* 1991; Ettl *et al.* 1991; Diederich & Whetten 1992; Kikuchi *et al.* 1992; Taylor *et al.* 1992). The predicted and observed most stable isomers obey the isolated pentagon rule: no pentagon shares an edge with another pentagon.

The geometry of fullerenes has been conventionally represented by drawings or models of polyhedra constructed from hexagons and pentagons. This geometry can be equally represented by the dual polyhedra: each three-connected vertex corresponds to a triangular facet, and each pentagon or hexagon to a five- or six-connected vertex. Polyhedra constructed from equilateral triangles are called deltahedra (Cundy & Rollet 1954). The particular class of deltahedra consisting of 12 five-vertices (V_5) and some number of six-vertices (V_6) was analysed to account for the symmetry of icosahedral viruses and to predict polymorphic forms of assembly for the coat proteins of these viruses (Caspar & Klug 1962, 1963). Possible designs for deltahedra can be systematically explored by considering the ways in which a plane equilateral triangular net can be cut and folded to form a polyhedron. A utility of the deltahedral representation of non-icosahedral surface lattices, such as many interesting higher fullerenes, is that the symmetry relations of the component trigonal units can be clearly visualized in the unfolded deltahedral lattice net.

2. Quasi-equivalence revisited

Quasi-equivalence was conceived to describe ways in which large numbers of identical protein subunits could build closed containers of predetermined size such as virus capsids by a 'self-assembly' process (Caspar & Klug 1962). Self-assembly presumes specificity of bonding among the structural units. If the same contacts between neighbouring units were used over and over again, in exactly the same way, identical units would be equivalently related and the completed assembly would have some kind of well-defined symmetry: this idea led to the prediction that rod-shaped viruses should have helical symmetry, and 'spherical' viruses might have tetrahedral, octahedral, or icosahedral symmetry (Crick & Watson 1956). Icosahedral symmetry, which was recognized by X-ray crystallography to be the underlying plan for some small isometric virus particles (Klug & Caspar 1960), requires 60, and only 60, equivalent chiral subdivisions. By 1962 chemical studies on two small icosahedral viruses had indicated a count of more than 60 identical protein molecules; and electron microscopy of some larger icosahedral viruses had revealed regular surface arrays of morphological units which were not multiples or submultiples of 60. These observations posed two interrelated questions. Why is icosahedral symmetry preferred? What are the possible designs for an icosahedral shell constructed by regular bonding of a multiple of 60 chiral structural subunits? Anticipation of the answers to these questions was critical to their formulation. The analogy drawn between icosahedral virus particle architecture and Buckminster Fuller's frequency modulated icosageodesic domes (Marks 1960) was the anticipatory key.

Fuller's dome designs involve the subdivision of the surface of the sphere into

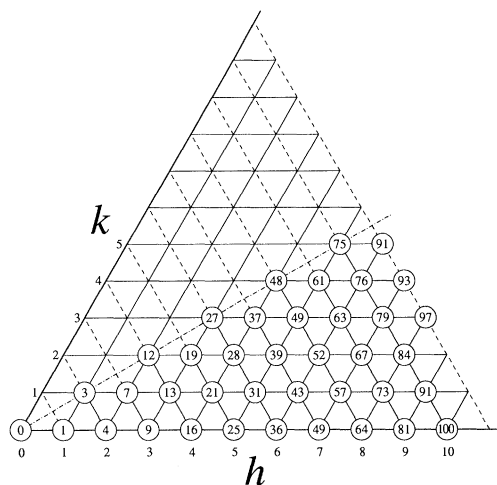


Figure 1. Triangulation numbers $T = (h^2 + hk + k^2)$ represented on an equilateral triangular net. An icosadeltahedron (see figure 2) with a five-fold vertex at the origin of this net and a neighbouring five-fold vertex at a lattice point of index h, k will have $\Delta = 20T$ triangular facets, $V_6 = 10(T-1)$ six-connected vertices, and $V_5 = 12$ five-vertices.

nearly equivalent facets arranged with icosahedral symmetry. If identical protein molecules were similarly packed in each geodesic facet, they would then be quasi-equivalently related. Geometrically, the quasi-equivalence could be measured from the variations in the size and shape of the nearly equal geodesic facets; at the molecular level, the same contact points between protein subunits could be used over and over again, but the units themselves or the bonds between them would have to be deformed in slightly different ways in the symmetrically distinct but quasi-equivalent positions. Arrangements that minimize the variation in subunit conformation and bonding should represent minimum energy designs for proteins selected to self-assemble in closed shells containing many molecules.

Possible designs for closed containers built of units that maintain the same pattern of nearest neighbour contacts can be represented by folding plane lattices into polyhedra in various ways, conserving the edge-to-edge connections of the plane facets. Pawley (1962) had shown that only plane lattices with square or equilateral triangular facets, having four- or six-fold rotational symmetry respectively, can be regularly folded onto the surface of convex polyhedra. It is evident that the smallest range of variation in dihedral angles is obtained if a six-connected vertex, V_6 , of the equilateral triangular net is transformed into a five-connected vertex, V_5 . If only V_5 s are allowed on folding the triangular net into a deltahedron, then by Euler's law, $V_5 = 12$ and the number of facets $\Delta = 20 + 2V_6$. The range of quasi-equivalent variation in the dihedral angles of such a deltahedron will be a minimum if the 12 V_5 s are all equivalently related, which requires icosahedral symmetry. This reasoning appeared to account for the selective advantage of icosahedral surface lattices for the construction of virus capsids from some large number of identical protein subunits (Casper & Klug 1962).

All the possible icosahedral surface lattice designs were enumerated by counting the ways in which the equilateral triangular net could be folded into polyhedra with icosahedral symmetry (called 'icosadeltahedra'). The vector between a neighbouring pair of V_5 s of any icosadeltahedron must be a lattice vector of the triangular net.

Since the 12 V_5 s are equivalent, the indices (h, k) of the vectors between a lattice point chosen as origin and any point of index (h, k) define all possible icosahedral surface lattices (figure 1). This way of counting is complete and non-redundant (Goldberg 1937; Caspar & Klug 1963). The number of triangular facets in an icosadeltahedron is $\Delta = 20T$, where the triangulation number $T = (h^2 + hk + k^2)$, and the number of $V_6 = 10(T - 1)$, or $V_5 + V_6 = 10T + 2$. If $h > k \neq 0$, the icosadeltahedron is chiral, and the pair of vectors (h, k) and (k, h) correspond to enantiomorphs. Figure 2 illustrates models of icosadeltahedra for the first five possible triangulation numbers ($T = 1, 3, 4, 7, 9$) built in 1962 from Geodestix components designed by Buckminster Fuller. As models for the design of virus capsids, each deltahedral facet could correspond to a quasi-symmetric trimer of identical, enantiomorphic protein molecules. As models for fullerenes, each deltahedral facet could represent a trivalent carbon atom with quasi or strict three-fold symmetry.

Protein molecules designed to self-assemble into icosahedral capsids of pre-determined size may assemble into polymorphic surface lattices of lower symmetry. Some virus capsid proteins may form tubular structures which have a diameter and surface structure similar to the icosahedral particles. Figure 3 illustrates how the $T = 4$ icosadeltahedron of figure 2, with $\Delta = 80$ and point group symmetry I_h , could be transformed into a $\Delta 80$ with D_{5h} symmetry by dividing the structure into two halves perpendicular to a five-fold axis and rejoining after rotating by one unit vector. The deltahedral cap can also be extended by adding rings of V_6 connectors to form a tube of any length. The tube design can be defined by the indices h, k of the circumferential vector; for the tube shown in figure 3, the indices $h, k = 10, 0$.

The design of the elongated heads of T -even bacteriophage is based on a chiral deltahedral surface lattice with D_5 symmetry. Mutants of these bacteriophage produce a wide variety of tubular structures built from hexamers of the major capsid protein arranged in cylindrical surface lattices (Yanagida *et al.* 1970). Under some conditions multilayered polyheads are formed, where an innermost tube of diameter *ca.* 40 nm appears to nucleate an assembly of successive layers. The inner tubes have somewhat variable diameters with circumferential vectors mostly within a narrow range of indices $h, k \approx 10, 6-12, 7$. Morphogenesis of the T -even bacteriophage head is a complex process, involving a number of structural and regulatory proteins (Black *et al.* 1992), but the assembled structures have quite regular surface lattice designs.

Considering the chemical complexity of even the simplest icosahedral viruses, it is remarkable that the icosadeltahedral surface lattices representing quasi-equivalent packing of identical molecules accounts so well for the morphology of such a wide variety of structures. The prediction of the quasi-equivalence theory (Caspar & Klug 1962) that the regular icosahedral virus capsids could be built of $60T$ identical protein molecules connected so as to form 12 pentamers and $10(T - 1)$ hexamers in an icosahedral surface lattice has been definitely established for the class of viruses with triangulation number $T = 3$, some of whose atomic structures have been solved by X-ray crystallography (Rossmann & Johnson 1989; Harrison 1991).

Larger icosahedral viruses that have been structurally well characterized do not obey the simple quasi-equivalence rule. For example, adenovirus capsids, for which $T = 25$, are built of 240 hexons (six-coordinated units) that are trimers of the major structural protein, and the 12 pentons consist of a different protein (Burnett 1984). Polyomavirus capsids, for which $T = 7$, are built of a single major structural protein,

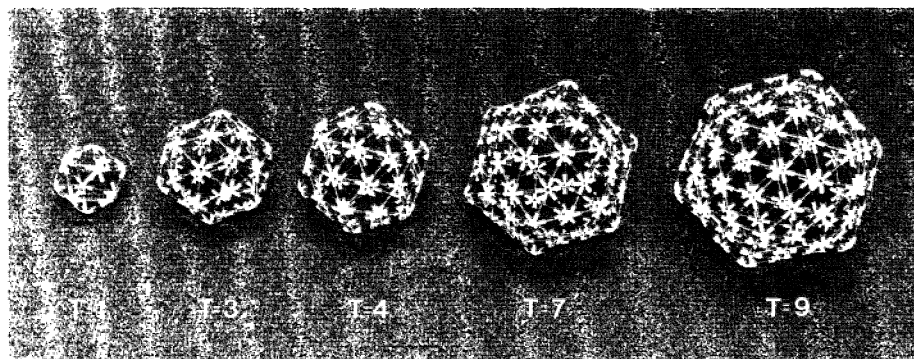


Figure 2. Models of icosadeltahedra for the first five possible triangulation numbers (built from Geodestix components).

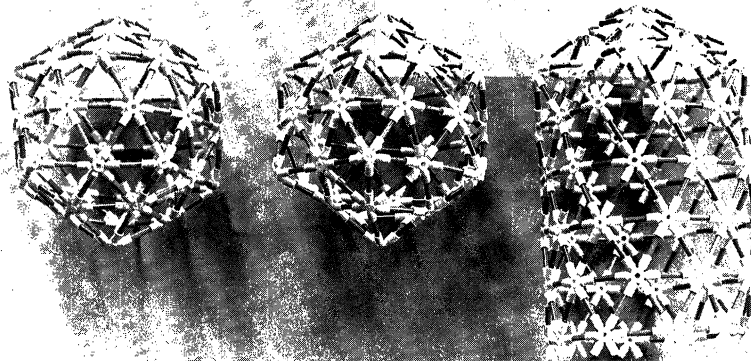


Figure 3. Polymorphism of deltahedral surface lattices. The $T = 4$ icosadeltahedron at the left ($\Delta 80$, point group I_h) is transformed to a $\Delta 80$ with D_{5h} symmetry (middle). At the right, the half-icosahedral cap defined by the $h, k = 10, 0$ circumferential vector has been extended by adding rings of 10 V_6 connectors. The bottom of this tube could be capped symmetrically (as for the $\Delta 80$ models) or asymmetrically using the $h, k = 10, 0$ cap shown in figure 4 or the two other $h, k = 10, 0$ caps listed in table 1.

but the 60 hexavalent units are pentamers, chemically identical to the 12 pentavalent pentamers (Rayment *et al.* 1982). Packing of the pentamers in hexagonal slots has been explained by determination of the molecular structure of the simian polyomavirus capsid (Liddington *et al.* 1991), which revealed a highly adaptable protein molecule with extended arms that can form regular contacts in symmetrically very different environments. The adaptability of such versatile protein molecules (Harrison 1991; Caspar 1992) goes beyond the rather modest degree of adjustment postulated for quasi-equivalently connected protein subunits of simple icosahedral virus capsids.

Carbon, although remarkable in the variety of structures that it can form, displays modest adjustability in the configuration of its bonds. Trivalent carbon in graphite can have D_{3h} symmetry, but in fullerene shells only C_{3v} , C_3 , C_{1v} and C_1 symmetry are

possible and the range of variation in bond distances and angles are limited. Thus, trivalent carbon atoms in fullerene shells conform to the geometrical postulates of the quasi-equivalence theory and the arrangement of the carbon atoms can be represented by the surface lattice of facets of a corresponding deltahedron. Any deltahedron built with 12 V_5 s represents a possible fullerene shell and those with all vectors between neighbouring V_5 pairs equal to or greater than $h, k = 1, 1$ satisfy the isolated pentagon rule. Analysis of the possible design of the higher fullerenes by Manolopoulos & Fowler (1992) has revealed a complex polyhedral stereochemistry which can be illustrated by deltahedral surface lattice nets.

Considering the polymorphism possible for units that could form icosahedral surface lattices, it was evident in 1962 (figure 3) that any icosadeltahedron could be divided into two equal halves in three different ways defined by a circumferential vector about an axis of five-, three- or two-fold symmetry, and that additional V_6 s could be added to form cylindrical extensions. Furthermore, it was found that any cylindrical lattice formed from the equilateral triangular net (of unit edge length) with a circumferential vector of length $(h^2 + hk + k^2)^{1/2}$ equal or greater than that for $h, k = 5, 0$ could be capped with six V_5 s. Thus, possible non-icosahedral deltahedra could be identified by cataloging the lattice vectors among six V_5 s that could cap each circumferential vector and connecting a pair of caps to a corresponding cylindrical section. In this way, deltahedra with no rotational symmetry were constructed, but 30 years ago the systematic enumeration of the myriad of designs for deltahedra with 12 V_5 s and large numbers of V_6 s appeared to be an unrewarding exercise. Discovery of the higher fullerenes has now made this classification an enlightening investigation.

3. Deltahedra unfolded

Just as any cylindrical surface lattice formed from the triangular net with a circumferential vector for which $(h^2 + hk + k^2) \geq 25$ can be capped with six V_5 s, so too can any deltahedron with 12 V_5 s be unfolded along the direction of a circumferential vector that delimits a pair of six V_5 caps. Figure 4 illustrates the unfolding and refolding of the chiral $\Delta 76$ deltahedron in the direction of the $h, k = 10, 0$ circumferential vector. This $\Delta 76$ with D_2 symmetry corresponds to the chiral C_{76} isolated and spectroscopically characterized by Ettl *et al.* (1991), and their notation for identifying the 19 carbon atoms in the asymmetric unit is followed in figure 4. The differences in the environments of the facets which distinguish the pyracylene, corrannulene and pyrene sites can be identified more readily in the unfolded net than in pictures of polyhedral models.

Unfolding $\Delta 76 D_2$ along the $h, k = 10, 0$ circumferential vector is not unique. In figure 5, the 11 symmetrically distinct ways of unfolding $\Delta 76 D_2$ are illustrated, together with the six ways of unfolding the tetrahedrally symmetric $\Delta 76 T_d$ isomer. In this figure, the boundaries of the surface lattice net are marked by the vectors between nearest neighbour V_5 s, rather than along the edges of triangular facets, as in figure 4.

Relations among possible fullerene surface lattices categorized by Manolopoulos & Fowler (1992) can be illustrated by deltahedral nets. For example, any deltahedron can be subtriangulated by applying any triangulation number (figure 1) to increase the number of facets by the factor T . Triangulating by $T = 3$ corresponds to Fowler's leap-frog rule. Any deltahedron circumscribed by a circumferential vector h, k can be

Deltahedral views of fullerene polymorphism

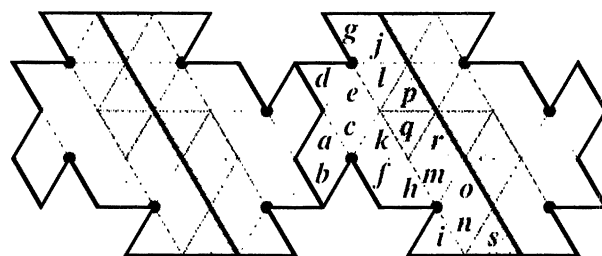
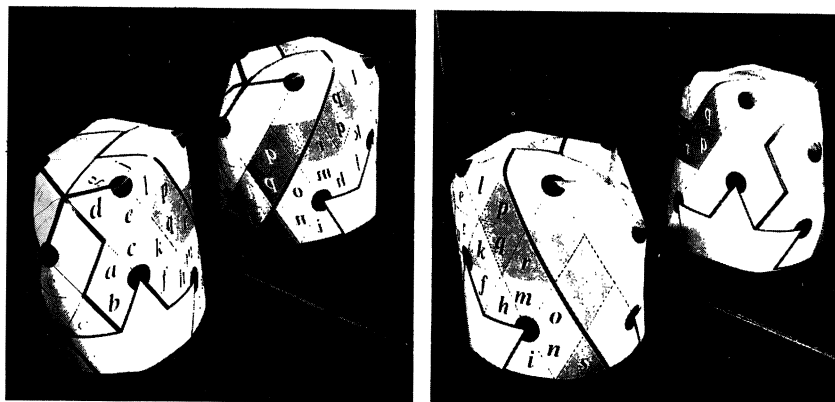

 $\Delta_{76} \quad D_2 \quad h, k = 10, 0$


Figure 4. Deltahedral surface lattice for the chiral Δ_{76} with D_2 symmetry, illustrated for the $h, k = 10, 0$ circumferential vector. An asymmetric unit of this surface lattice, consisting of the 19 facets labelled a – s , has been marked with a bold outline. The labelling of the facets follows the notation of Ettl *et al.* (1991) for the carbon atoms of the chiral C_{76} . Facets a – i (white) correspond to pyracylene sites, j – q (light grey) to corrannulene sites, and p – s (dark grey) to pyrene sites. The three classes of two-fold axes are located between the a – a , r – r , and s – s facets. The opened-out lattice (top) is folded into $\Delta_{76} D_2$ by connecting the pair of a facets related by the $h, k = 10, 0$ circumferential vector to form a tube segment which is capped by forming the V_5 s marked by black circles. Two views of the half-capped tubular segment are shown with their mirror images (bottom). Folding the surface lattice inside-out would have produced the mirror-image structure.

elongated following the idea of Fowler's cylinder extension rule, in steps of n added V_6 s (or $2n\Delta$ s) where n is the common factor of h and k . Furthermore, for circumferential vectors with a common factor higher than the axial symmetry of the caps, twisting the caps about the cylinder axis can generate a different deltahedron.

Some of the relations among the 11 smallest deltahedra that obey the isolated pentagon rule (IPDs) are classified in figure 6. For Δ_{60} – Δ_{76} , all circumferential vectors are listed that divide each deltahedron into two caps with six V_5 s each. For the five isomers of Δ_{78} , only those representations of the unfolded deltahedron nets are listed that can be derived by cylindrical extension or alternate combination of the caps of a smaller deltahedron. In general, a tube defined by a circumferential vector h, k can be capped in more than one way. A more complete listing of possible cap designs for tubes larger than those included in table 1 could be produced by enumerating the circumferential vectors for the higher fullerenes catalogued by Manolopoulos & Fowler (1992).

Of the deltahedra listed in figure 6, $\Delta_{60} I_h$, $\Delta_{72} D_{6d}$, and $\Delta_{78} D_{3h}$ can be respectively derived by the $T = 3$ triangulation as follows: Δ_{60} from Δ_{20} the

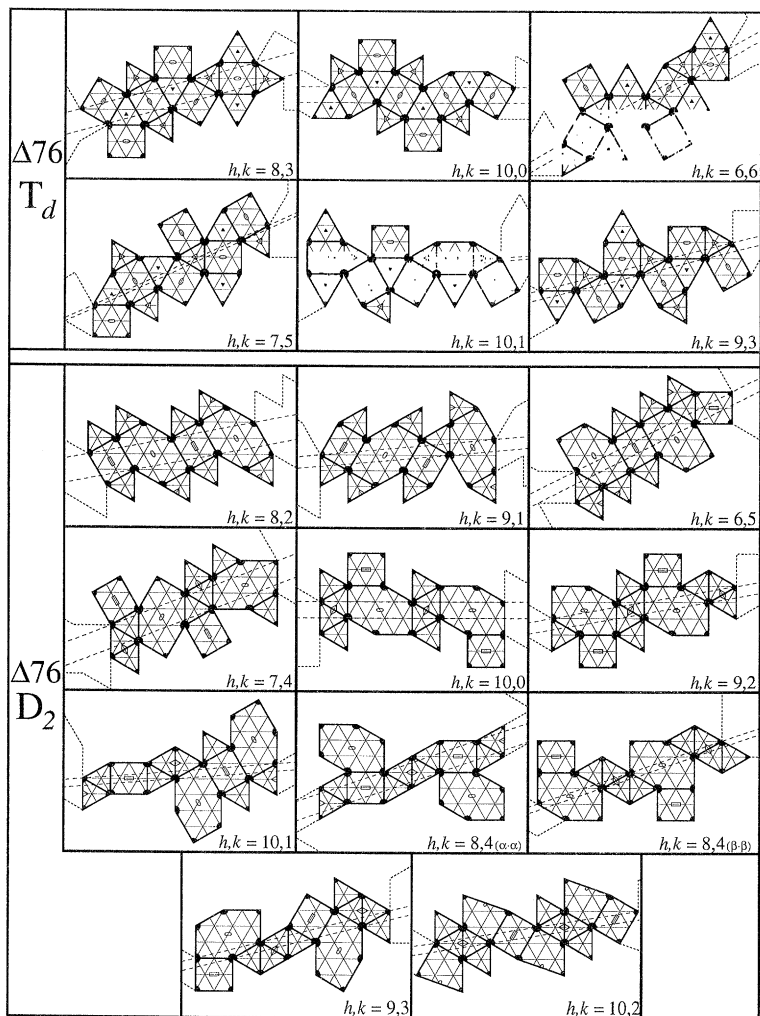


Figure 5. Unfolding of the tetrahedral T_d and chiral D_2 isomers of $\Delta 76$ according to the possible circumferential vectors that divide the deltahedra into two caps. The pair of circumferential vectors at the boundary of each tubular segment (which contains no V_5 s) are marked by dashed lines. V_5 lattice points are indicated by black circular sectors and the vectors between nearest neighbour V_5 s are marked by bold lines. The dotted lines indicate how the two ends of the circumferential vectors are joined to form the tubular segment. Folding only along the vectors between V_5 s would produce a polyhedron with the marked polygons as facets; whereas folding only along edges of the triangular net produces the deltahedron (cf. figure 4). The symmetrically distinct rotational axes for the T_d and D_2 point groups are marked with distinguishing shapes. Circumferential vectors have been chosen with $h > k$ and are arranged in order of increasing length $(h^2 + hk + k^2)^{1/2}$. (Interchanging h and k produces the enantiomorphic net for the D_2 surface lattices.) Increasing the separation of the pairs of circumferential vectors by addition of V_6 s leads to cylinder extension generating higher deltahedra (cf. table 1).

icosahedron; $\Delta 72$ from $\Delta 24$, the hexagonal antiprism (which can be derived from the icosahedron by adding two V_6 s in extension along a two-fold axis); and $\Delta 78$ from $\Delta 26$, derived from the icosahedron by addition of three V_6 s extended along a three-fold axis. In turn, by extension, $\Delta 70$ derives from $\Delta 60$; $\Delta 74$ from $\Delta 70$; $\Delta 76 D_2$ from $\Delta 60$ and $\Delta 72$ by one path or from $\Delta 70$ by two different paths; and $\Delta 76 T_d$ from $\Delta 74$.

Point Δn Group	Index h, k of Circumferential Vectors																	
	5,5	6,4	7,3	9,0	8,2	9,1	6,5	7,4	8,3	10,0	9,2	6,6	7,5	10,1	8,4	9,3	11,0	10,2
$\Delta 60$ I_h	$\alpha \cdot \alpha$			$\alpha \cdot \alpha$	$\alpha \cdot \alpha$													
$\Delta 70$ D_{5h}	$\alpha \cdot \alpha$					$\alpha \cdot \alpha$		$\alpha \cdot \alpha$		$\alpha \cdot \beta$								
$\Delta 72$ D_{6d}					$\alpha \cdot \alpha$			$\beta \cdot \beta$			$\alpha \cdot \alpha$		$\alpha \cdot \alpha$					
$\Delta 74$ D_{3h}								$\alpha \cdot \alpha$	$\alpha \cdot \alpha$	$\alpha \cdot \gamma$			$\alpha \cdot \alpha$	$\beta \cdot \beta$		$\alpha \cdot \alpha$		
$\Delta 76$ T_d								$\alpha \cdot \alpha$	$\alpha \cdot \alpha$		$\beta \cdot \beta$	$\alpha \cdot \beta$	$\beta \cdot \gamma$		$\alpha \cdot \beta$			
" D_2					$\alpha \cdot \alpha$	$\alpha \cdot \alpha$	$\alpha \cdot \alpha$	$\alpha \cdot \alpha$		$\alpha \cdot \alpha$	$\alpha \cdot \alpha$			$\delta \cdot \delta$	$\alpha \cdot \alpha$ $\beta \cdot \beta$	$\gamma \cdot \gamma$		$\alpha \cdot \alpha$
$\Delta 78$ D_{3h}				$\alpha \cdot \alpha$				$\beta \cdot \beta$						$\alpha \cdot \alpha$				
" C_{2v}						$\alpha \cdot \alpha$		$\alpha \cdot \beta$										
" $C_{2v'}$								$\alpha \cdot \alpha$										
" $D_{3h'}$								$\alpha \cdot \alpha$				$\beta \cdot \beta$	$\gamma \cdot \gamma$			$\beta \cdot \beta$		
" D_3				$\alpha \cdot \alpha$														

Figure 6. Circumferential vectors of deltahedra with isolated pentameric vertices (IPAs). All circumferential vectors from $h, k = 5, 5$ to $10, 2$ are listed in order of increasing length $(h^2 + hk + k^2)^{\frac{1}{2}}$. This listing indicates possible designs for fullerene tubes that can be capped with isolated pentamers. No such caps are possible for circumferential vectors $h, k = 6, 4$ or $7, 3$; for longer circumferential vectors, more than one arrangement of six V_5 s may cap a tube segment. Symmetrically distinct caps are sequentially designated $\alpha, \beta, \gamma, \delta, \dots$, as they are listed for each h, k vector for progressively larger IPAs. Surface lattice nets for the $\Delta 76$ and $\Delta 78$ isomers are illustrated in figures 5 and 6 respectively.

Furthermore, as is evident from figures 4 and 5, the chiral $\Delta 76 D_2$ can be converted into the tetrahedral $\Delta 76 T_d$ by shifting the top cap related by the $10, 0$ circumferential vector one lattice unit to the left. Shifting two units to the left generates the D_2 enantiomer. Continuing this shifting three or four steps brings a V_5 pair one lattice unit apart, which violates the isolated pentagon rule, and five steps comes back by symmetry to a starting point. Cylinder extension, by adding V_6 s, can also lead to apposition of V_5 s that violates the isolated pentamer rule, indicated for example by the blank entries for $\Delta 72$ and $\Delta 74$ in the column for the $9, 1$ circumferential vector in figure 6.

The interrelation of the five isomers of $\Delta 78$ is illustrated in figure 7. At the left, unfolded surface lattices are drawn as in figure 5 for selected circumferential vectors from the listing in figure 6. In the centre, projected views of the fullerene polyhedra are compared with their deltahedra duals in the same orientation. At the right, surface lattices for the four mirror-symmetric $\Delta 78$ isomers are drawn with boundaries marked along the edges of triangular facets as in figure 4. These unfolded nets emphasize the invariant and variable aspects of the polymorphic interchange among the isomers of C_{78} $D_{3h} \rightleftharpoons C_{2v} \rightleftharpoons C_{2v'} \rightleftharpoons D_{3h'}$ as described by Diederich *et al.* (1991). Switching among these isomers by rotation of a C_2 -unit in a pyracylene rearrangement, following the mechanism proposed by Stone & Wales (1986), is illustrated in figure 7 by the step-wise reorientation of the three shaded pairs of triangular facets. This local reorientation leads to the interchange of a V_5 and V_6 pair in the surface lattice. In contrast, there is no simple interchange between the chiral D_3 isomer and any of the four mirror-symmetric isomers. The $\Delta 78 D_{3h}$ can be transformed to the D_3 isomer shown at the top of figure 7 by shifting the upper cap defined by the $9, 0$ circumferential vector one unit to the right, or to its enantiomer by the opposite shift. However, for C_{78} this would correspond to the improbable breaking and reforming of 18 C-C bonds.

NMR spectra of purified C_{78} obtained in different laboratories (Diederich *et al.* 1991;

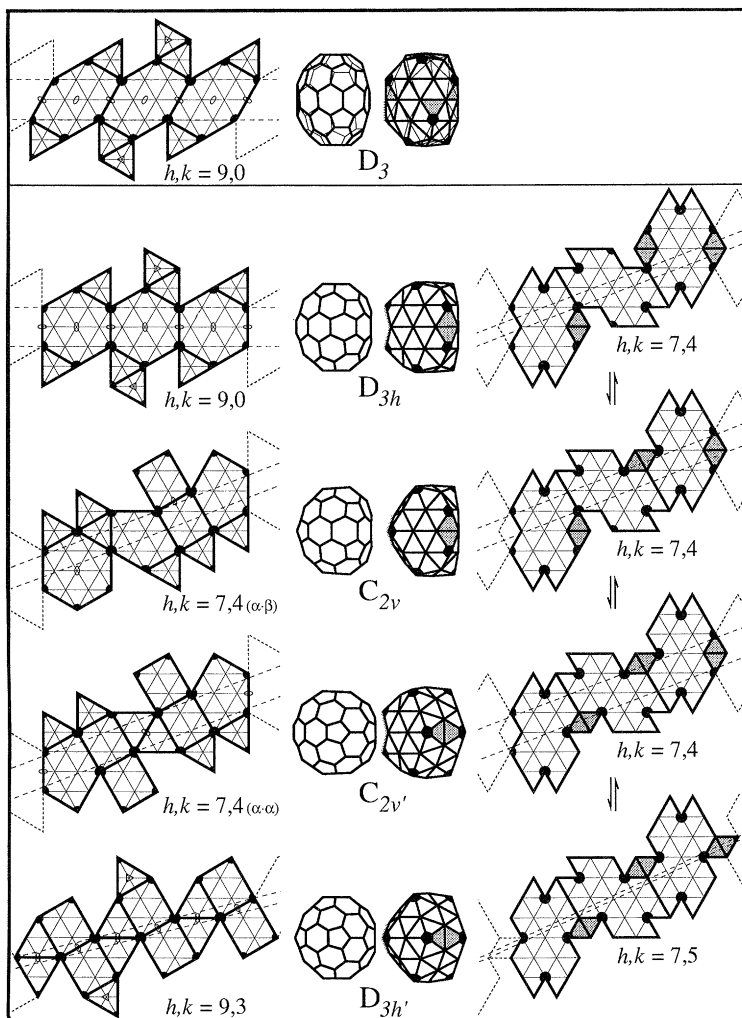


Figure 7. $\Delta 78$ isomers. The unfolded surface lattice nets at the left are drawn with boundaries along the vectors between nearest neighbour V_5 s which are marked by the black circular sectors, whereas the boundaries for the nets at the right are along the edges of deltahedral facets. The projected views of the fullerene polyhedra and deltahedra duals in the centre column are all oriented with a corresponding two-fold axis horizontal. For the four mirror-symmetric isomers, there is one mirror plane in the plane of projection and an orthogonal horizontal one. Marking the symmetry elements for each isomer on the deltahedral surface lattice net defines the asymmetric unit.

Kikuchi *et al.* 1992; Taylor *et al.* 1992) indicate variable proportions of the isomers D_3 , C_{2v} and $C_{2v'}$. The spectra expected for each isomer can be predicted by enumerating the number of symmetrically distinct carbon atoms in the asymmetric unit and noting their local environment (Fowler *et al.* 1991). The deltahedral facets composing the asymmetric units of each $\Delta 78$ isomer in figure 7 could be labelled as in figure 4, distinguishing the pyracylene, corrannulene and pyrene sites.

The unfolded deltahedral nets provide a convenient way to illustrate the environments of the different carbon atoms in the asymmetric unit of higher fullerenes, in particular those of relatively low symmetry. The interrelation among fullerenes of different size and among various isomers can also be displayed by such

nets. In particular, interconversion pathways that involve local reorientations at relatively distant sites can be simply mapped. Furthermore, the classification of the deltahedra according to their circumferential vectors provides a systematic way to enumerate how nanotubes can be capped, and how multilayered tubes (Iijma 1991) or shells (McKay *et al.* 1992) can be successively encapsulated.

I thank Eric Fontano for preparing the computer graphics diagrams and Marie Craig for photographic assistance. This work has been supported by United States Public Health Service Grant CA47439 from the National Cancer Institute.

References

- Black, L. F., Showe, M. K. & Steven, A. C. 1992 Morphogenesis of the T4 head. In *Bacteriophage T4* (ed. T. Karam & F. A. Eiserling), 2nd edn. Washington, D.C.: American Society for Microbiology.
- Burnett, R. M. 1984 Structural investigations of hexon, the major coat protein of adenovirus. In *Biological macromolecules and assemblies (Volume 1: Virus structures)* (ed. F. A. Jurnak & A. McPherson), pp. 377–385. New York: John Wiley & Sons.
- Caspar, D. L. D. 1992 Virus structure puzzle solved. *Current Biol.* **2**, 169–171.
- Caspar, D. L. D. & Klug, A. 1962 Physical principles in the construction of regular viruses. *Cold Spring Harbor Symp. Quant. Biol.* **27**, 1–24.
- Caspar, D. L. D. & Klug, A. 1963 Structure and assembly of regular virus particles. In *Viruses, nucleic acids, and cancer*, pp. 27–39. Baltimore: Williams & Wilkins.
- Crick, F. H. C. & Watson, J. D. 1956 The structure of small viruses. *Nature, Lond.* **177**, 473–475.
- Cundy, H. M. & Rollett, A. P. 1954 *Mathematical Models*, 2nd edn. Oxford: Clarendon Press.
- Diederich, F., Whetten, R. L., Thilgen, C., Ettl, R., Chao, I. & Alvarez, M. M. 1991 Fullerene isomerism: Isolation of C_{2v} - C_{78} and D_3 - C_{78} . *Science, Wash.* **254**, 1768–1770.
- Ettl, R., Chao, I., Diederich, F. & Whetten, R. L. 1991 Isolation of C_{76} , a chiral (D_2) allotrope of carbon. *Nature, Lond.* **353**, 149–153.
- Fowler, P. W., Batten, R. C. & Manolopoulos, D. E. 1991 The higher fullerenes: a candidate for the structure of C_{78} . *J. chem. Soc. Faraday Trans.* **87**, 3103–3104.
- Fuller, R. B. 1963 *Ideas and integrities*. Englewood Cliffs, New Jersey: Prentice-Hall.
- Goldberg, M. 1937 A class of multi-symmetric polyhedra. *Tôhoku Math. J.* **43**, 104–108.
- Harrison, S. C. 1991 What do viruses look like? *Harvey Lectures* **85**, 123–148.
- Iijma, S. 1991 *Nature, Lond.* **354**, 56–58.
- Kikuchi, K., Nakahara, N., Wakabayashi, T., Suzuki, S., Shiromaru, H., Miyake, Y., Saito, K., Ikemoto, I., Kainosho, M. & Achiba, Y. 1992 NMR characterization of isomers of C_{78} , C_{82} and C_{84} fullerenes. *Nature, Lond.* **357**, 142–145.
- Klug, A. & Caspar, D. L. D. 1960 The structure of small viruses. *Adv. Virus Res.* **7**, 225–325.
- Kroto, H. W., Heath, J. R., O'Brien, S. C., Curl, R. F. & Smalley, R. E. 1985 C_{60} : Buckminsterfullerene. *Nature, Lond.* **318**, 162–164.
- Liddington, R. C., Yan, Y., Moulai, J., Sahli, R., Benjamin, T. L. & Harrison, S. C. 1991 Structure of simian virus 40 at 3.8-Å resolution. *Nature, Lond.* **354**, 278–284.
- Mackay, A. L. 1962 A dense non-crystallographic packing of equal spheres. *Acta crystallogr.* **15**, 916–918.
- Manolopoulos, D. E. 1991 Proposal of a chiral structure for the fullerene C_{76} . *J. chem. Soc. Faraday Trans.* **87**, 2861–2862.
- Manolopoulos, D. E. & Fowler, P. W. 1992 Molecular graphs, point groups, and fullerenes. *J. chem. Phys.* **96**, 7603–7614.
- Marks, R. W. 1960 *The dymaxion world of buckminster fuller*. New York: Reinhold.
- McKay, K. G., Kroto, H. W. & Wales, D. J. 1992 *J. chem. Soc. Faraday Trans.* **88**, 2815–2821.
- Pawley, G. S. 1962 Plane groups on polyhedra. *Acta crystallogr.* **15**, 49–53.
- Phil. Trans. R. Soc. Lond. A* (1993)

- Rayment, I., Baker, T. S., Caspar, D. L. D. & Murakami, W. T. 1982 Polyomavirus capsid structure at 22.5 Å resolution. *Nature, Lond.* **295**, 110–115.
- Rossmann, M. G. & Johnson, J. E. 1989 Icosahedral RNA virus structure. *A. Rev. Biochem.* **58**, 533–573.
- Stone, A. J. & Wales, D. J. 1986 Theoretical studies of icosahedral C₆₀ and some related species. *Chem. Phys. Lett.* **128**, 501–503.
- Taylor, R., Langley, G. J., Dennis, T. J. S., Kroto, H. W. & Walton, D. R. M. 1992 A mass spectrometric-NMR study of fullerene-78 isomers. *J. chem. Soc. Chem. Commun.*, 1043–1046.
- Yanagida, M., Boy de la Tour, E., Alff-Steinberger, C. & Kellenberger, E. 1970 Studies on the morphopoiesis of the head of bacteriophage T-even. VII. Multilayer polyheads. *J. molec. Biol.* **50**, 35–58.

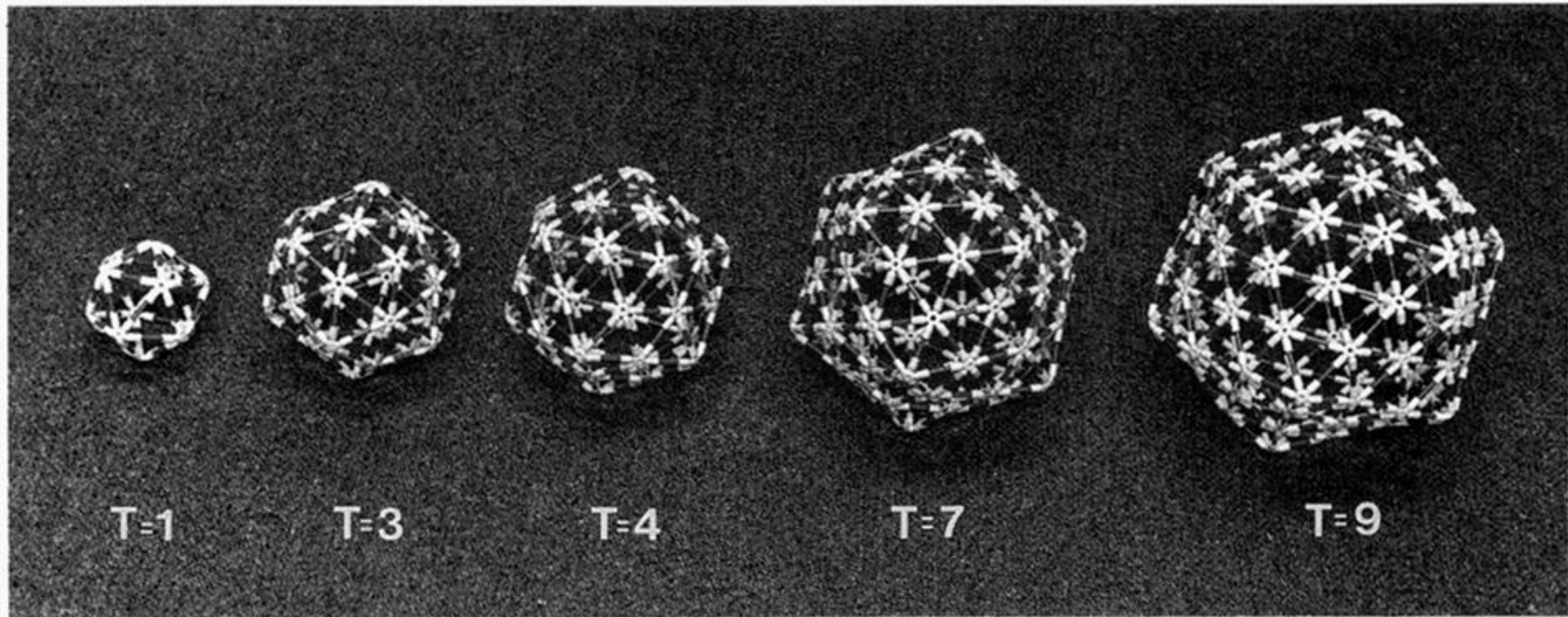


Figure 2. Models of icosadeltahedra for the first five possible triangulation numbers (built from Geodestix components).

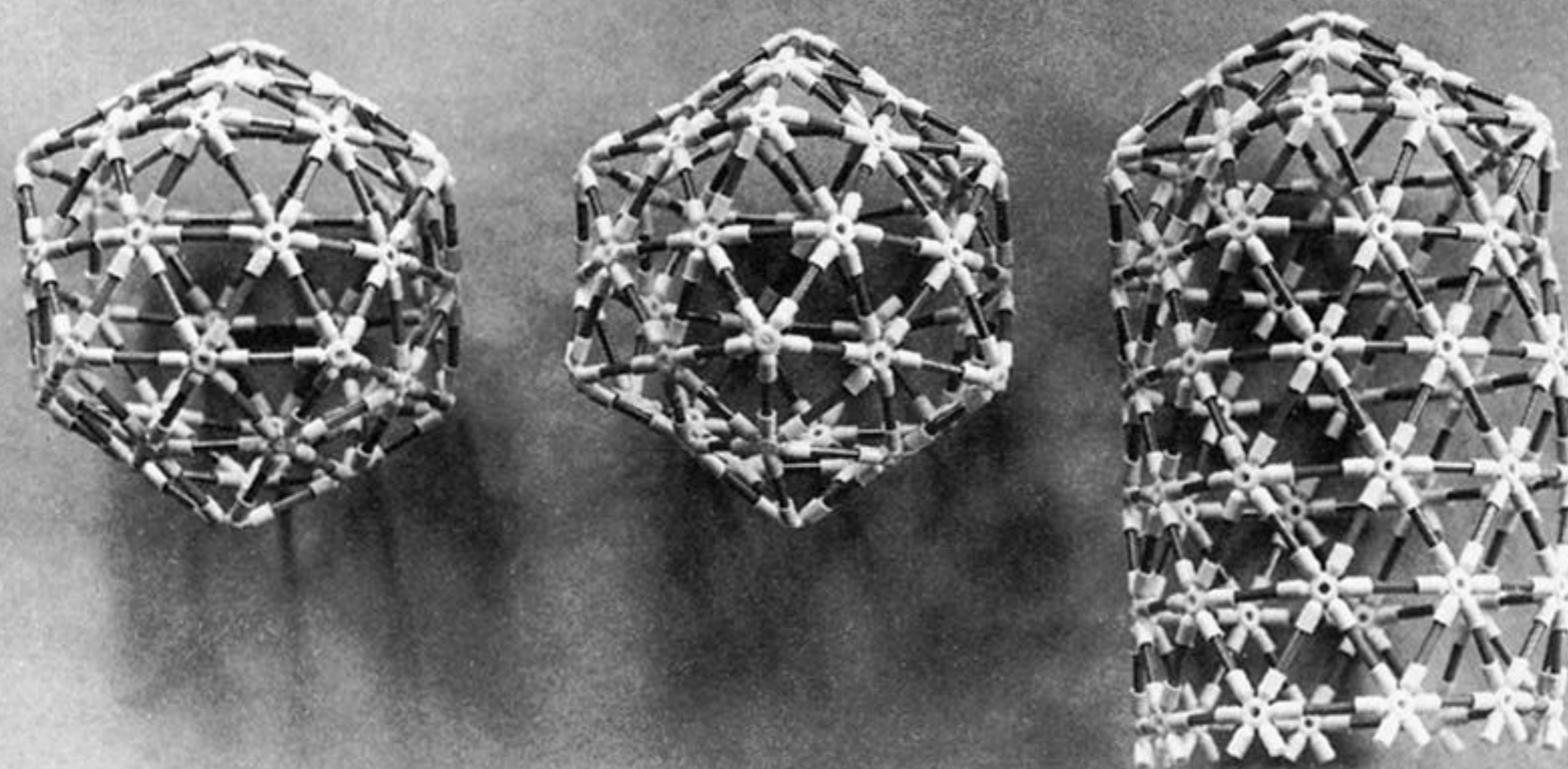
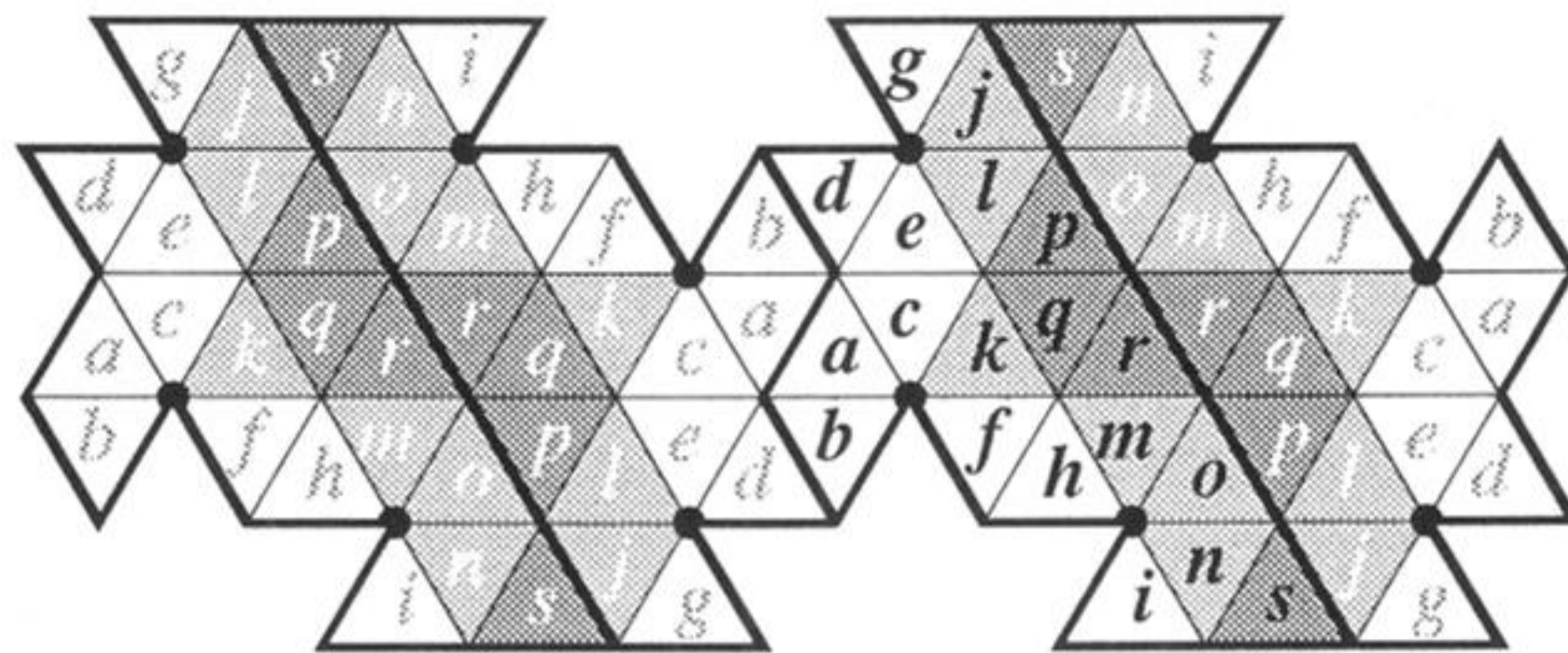


Figure 3. Polymorphism of deltahedral surface lattices. The $T = 4$ icosadeltahedron at the left ($\Delta 80$, point group I_h) is transformed to a $\Delta 80$ with D_{5h} symmetry (middle). At the right, the half-icosahedral cap defined by the $h, k = 10, 0$ circumferential vector has been extended by adding rings of 10 V_6 connectors. The bottom of this tube could be capped symmetrically (as for the $\Delta 80$ models) or asymmetrically using the $h, k = 10, 0$ cap shown in figure 4 or the two other $h, k = 10, 0$ caps listed in table 1.



$\Delta 76 \quad D_2 \quad h, k = 10, 0$

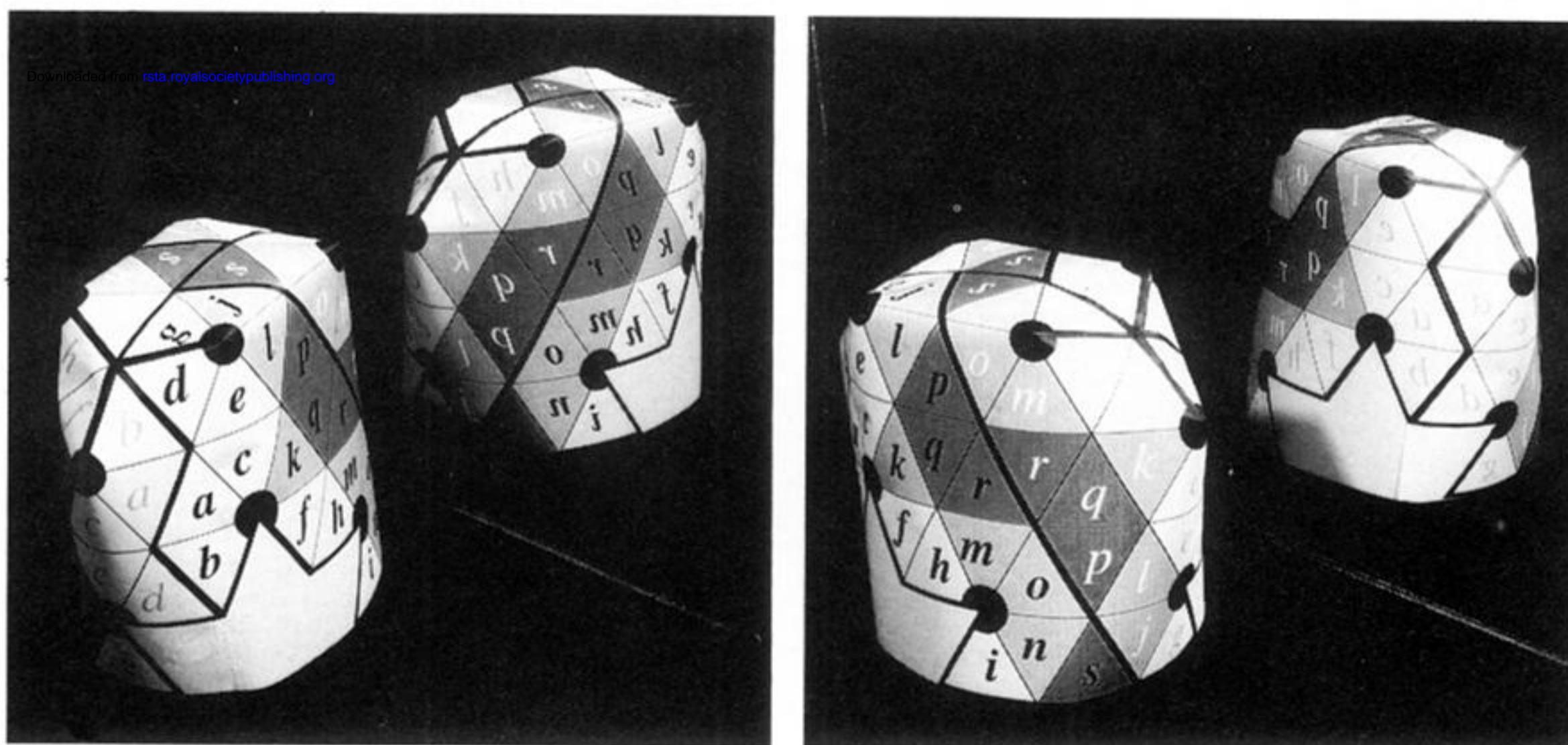


Figure 4. Deltahedral surface lattice for the chiral $\Delta 76$ with D_2 symmetry, illustrated for the $h, k = 10, 0$ circumferential vector. An asymmetric unit of this surface lattice, consisting of the 19 facets labelled a – s , has been marked with a bold outline. The labelling of the facets follows the notation of Ettl *et al.* (1991) for the carbon atoms of the chiral C_{76} . Facets a – i (white) correspond to pyracylene sites, j – q (light grey) to corrannulene sites, and p – s (dark grey) to pyrene sites. The three classes of two-fold axes are located between the a – a , r – r , and s – s facets. The opened-out lattice (top) is folded into $\Delta 76 D_2$ by connecting the pair of a facets related by the $h, k = 10, 0$ circumferential vector to form a tube segment which is capped by forming the V_5 s marked by black circles. Two views of the half-capped tubular segment are shown with their mirror images (bottom). Folding the surface lattice inside-out would have produced the mirror-image structure.